Fast Track Communications

IOP Publishing Journal of Physics A: Mathematical and Theoretical

J. Phys. A: Math. Theor. **47** (2014) 492002 (10pp) doi:10.1088/1751-8113/47/49/492002

Fast Track Communication

Localisation and universal fluctuations in ultraslow diffusion processes

Aljaž Godec[1,2], Aleksei V Chechkin[1,3,4], Eli Barkai[5], Holger Kantz[4] and Ralf Metzler[1,6]

[1] Institute for Physics & Astronomy, University of Potsdam, D-14476 Potsdam-Golm, Germany
[2] National Institute of Chemistry, 1000 Ljubljana, Slovenia
[3] Institute for Theoretical Physics, Kharkov Institute of Physics and Technology, Kharkov 61108, Ukraine
[4] Max Planck Institute for the Physics of Complex Systems, Nöthnitzer Straße 38, D-01187 Dresden, Germany
[5] Department of Physics, Bar Ilan University, Ramat-Gan 52900, Israel
[6] Department of Physics, Tampere University of Technology, FI-33101 Tampere, Finland

E-mail: rmetzler@uni-potsdam.de

Received 22 October 2014
Accepted for publication 31 October 2014
Published 14 November 2014

Abstract

We study ultraslow diffusion processes with logarithmic mean squared displacement (MSD) $\langle x^2(t)\rangle \simeq \log^\gamma t$. Comparison of annealed (renewal) continuous time random walks (CTRWs) with logarithmic waiting time distribution $\psi(\tau) \simeq 1/(\tau \log^{1+\gamma}\tau)$ and Sinai diffusion in quenched random landscapes reveals striking similarities, despite the great differences in their physical nature. In particular, they exhibit a weakly non-ergodic disparity of the time-averaged and ensemble-averaged MSDs. Remarkably, for the CTRW we observe that the fluctuations of time averages become universal, with an exponential suppression of mobile trajectories. We discuss the fundamental connection between the Golosov localization effect and non-ergodicity in the sense of the disparity between ensemble-averaged MSD and time-averaged MSD.

Keywords: Sinai diffusion, anomalous diffusion, quenched energy landscape
PACS numbers: 72.20.Jv, 72.70.+m, 89.75.Da, 05.40.-a

(Some figures may appear in colour only in the online journal)

1. Introduction

Ever since Pearson's defining Letter to the Editor of 1905 [1], and Einstein's and Smoluchowski's mean free path studies [2], *random walks* have been used as a standard tool in approaching a multitude of nonequilibrium phenomena across disciplines [3–6]. Usually renewal random walks are used [5], in which jumps have no memory, reflecting the motion in an annealed environment [7]. This contrasts with random walks in quenched environments in which a particle progressively builds up correlations when it revisits locations with site-specific properties [7]. The prototype approach is based on Temkin's lattice model with site-dependent probabilities for jumping left or right [3, 8].

A great leap forward came with Sinai's study of a special case of Temkin's model in which a walker jumps from site x to $x \pm 1$ with the site-specific probability $p_x = \frac{1}{2}(1 \pm \varepsilon s_x)$ [9]. Here, the amplitude $0 < \varepsilon < 1$, and $s_x = \pm 1$ with probability 1/2 [3, 10]. Sinai diffusion can be viewed as a random walk in the quenched potential landscape created by a standard random walk. A simple argument for the temporal spreading in Sinai diffusion goes as follows [7]. To span a distance x from its starting point, the particle needs to cross an energy barrier of order $\sqrt{x}$ with activation time $\tau \sim \tau_1 \exp(\sigma\sqrt{x})$, where σ is a measure for the disorder strength versus the thermal energy and τ_1 a fundamental time scale. The distance covered by the walker during time t then scales as $x^2 \simeq \ln^4(t/\tau_1)$.

Sinai diffusion is related to random-field Ising models [11, 12] and helix-coil boundaries in random heteropolymers [13]. With the inherently quenched heterogeneity of biomolecules, Sinai-type models describe mechanical DNA unzipping [14], translocation of biopolymers through nanopores [15, 16], and molecular motors [16]. Ultraslow diffusion with mean squared displacement (MSD)

$$\langle x^2(t)\rangle \simeq 2K_\gamma \ln^\gamma t, \quad \gamma > 0, \tag{1}$$

in fact has a much wider scope in disordered systems of low dimension: e.g., in vacancy-induced motion [17], biased motion in exclusion processes [18], motion in ageing environments [19], compactification of paper [20] or grain [21], dynamics in glassy systems [22], record statistics [23], the ABC model [24], diffusion with exponential position dependence of the diffusivity [25], and dynamics in nonlinear maps [26]. Logarithmic diffusion (1) with $\gamma = 1/2$ also emerges in interacting many-particle systems in one dimension [27].

Previous work focused on ensemble-averaged observables. The routine observation of single-particle trajectories in the laboratory forces us to investigate time averages theoretically. Moreover, in real systems the landscape is often quenched, but the analysis of time averages has mostly relied on ideas valid for the annealed scenario [6, 28]. It was also found that quenched disorder can dramatically affect the statistics of time averages [29–31]. There thus exists a pressing need for theoretical results going beyond ensemble averages that would shed light on ergodic properties in systems with quenched disorder.

Here we report a comparative study of Sinai diffusion and ultraslow continuous time random walks (CTRWs) with superheavy-tailed waiting times [26, 32–34]. We study their time-averaged MSD and demonstrate the fundamental disparity between ensemble and time averages. These weakly non-ergodic behaviors [28, 35] are, up to a prefactor, identical for the two processes. We discuss why, despite the seeming similarity, the problems of ergodicities in annealed and quenched systems are very different. In addition, we unveil the *universal* exponential fluctuations of the time-averaged MSD of the CTRW process and provide numerical evidence of the Golosov localization effect for different disorder realizations in

Sinai diffusion. Concurrently, the PDF of the CTRW process is shown to be practically indistinguishable from that of Sinai diffusion.

2. Sinai diffusion

We start with the analysis of Sinai diffusion. In the continuum limit, its MSD reads [11, 36]

$$\widetilde{\langle x^2(t)\rangle} \simeq (61/180)\,\ln^4(t), \tag{2}$$

in scaled units. Here $\langle\cdot\rangle$ is an ensemble average over white Gaussian noise and $\widetilde{\ }$ a disorder average. Figure 1 shows the excellent agreement with our extensive simulations.

To simulate Sinai diffusion, we follow the approach of [36] based on a discrete-space Fokker–Planck equation for a particular realization of the random potential. Mapping the Fokker–Planck equation onto the corresponding (imaginary time) Schrödinger equation, we obtain the propagator as an expansion in eigenstates from diagonalization of the Schrödinger operator. From the disorder-averaged one-point and two-point propagators, we evaluate the time-averaged and ensemble-averaged MSDs (see also below). The results were averaged over 5000 realizations of the random potential with 10^8 time steps each [37].

Individual time series $x(t)$ garnered by modern single-particle tracking techniques or from simulations are typically evaluated in terms of the time-averaged MSD [6, 26]

$$\overline{\delta^2(\Delta)} = \frac{1}{t-\Delta}\int_0^{t-\Delta}[x(t'+\Delta)-x(t')]^2\,\mathrm{d}t', \tag{3}$$

with the lag time Δ and the length t of the time series. The overline $\overline{\ \cdot\ }$ denotes the time average. Averaging equation (3) over many trajectories embedded in different realizations of the disorder, we obtain

$$\widetilde{\left\langle\overline{\delta^2(\Delta)}\right\rangle} \sim \frac{1}{t-\Delta}\int_0^{t-\Delta}\left[\widetilde{\langle x^2(t'+\Delta)\rangle} + \widetilde{\langle x^2(t')\rangle} - 2\widetilde{\langle x(t')x(t'+\Delta)\rangle}\right]\mathrm{d}t', \tag{4}$$

where the two-point position correlation function

$$\widetilde{\langle x(t')x(t'+\Delta)\rangle} = \sqrt{\widetilde{\langle x^2(t'+\Delta)\rangle}\,\widetilde{\langle x^2(t')\rangle}}\times f(y) \tag{5}$$

is known from renormalization group calculations by Le Doussal *et al* [36], where $y = \ln(t'+\Delta)/\ln t'$ and

$$f(y) = \frac{72}{61y} - \frac{40}{61y^2} - \frac{180}{427y^3} + \frac{2045}{1281y^4} + \mathrm{e}^{y-1}\left(\frac{20}{61y^2} - \frac{80}{183y^3} - \frac{36}{61y^4}\right). \tag{6}$$

Inserting this into equation (4), we obtain our first main result, the time-averaged MSD:

$$\widetilde{\left\langle\overline{\delta^2(\Delta)}\right\rangle} \simeq \frac{3721}{17080}\ln^4(t)\frac{\Delta}{t} = \widetilde{\langle x^2(t)\rangle}\frac{549}{854}\frac{\Delta}{t}, \tag{7}$$

up to corrections of order $(\Delta/t)^2$ [37]. We observe in equation (7) the distinct disparity between the MSD (2) and its time-averaged analogue (7). In contrast to the logarithmic time dependence (2) for the MSD, the time-averaged MSD (7) grows *linearly* with the lag time Δ.

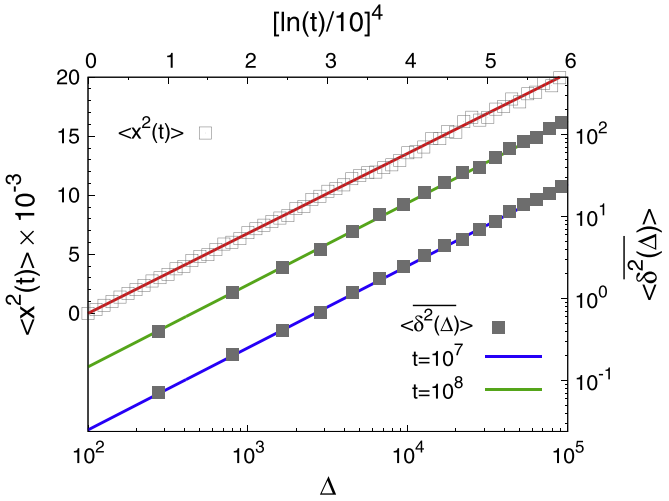

Figure 1. Ensemble-averaged (□, top and left axes) and time-averaged (■, bottom and right axes, for $t = 10^7$ and $t = 10^8$) MSD of Sinai diffusion. The simulations agree excellently with the analytical results (full lines) from equations (2) and (7). Note that we show $10^{-3}\langle x^2(t)\rangle$ such that for sufficiently long trajectories (long t in equation (7)), $\langle x^2\rangle \gg \overline{\delta^2}$.

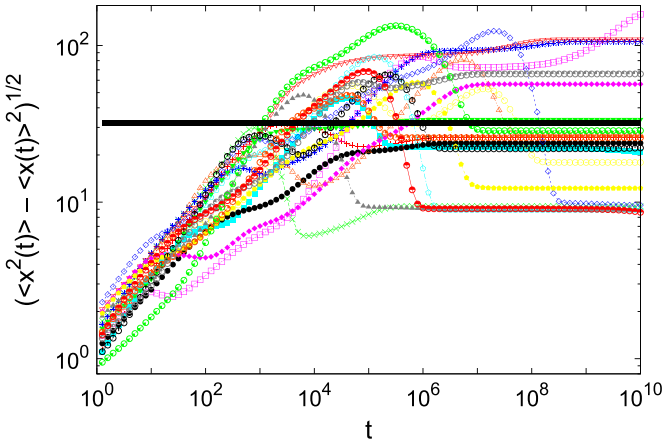

Figure 2. Standard deviation $[\langle x^2(t)\rangle - \langle x(t)\rangle^2]^{1/2}$ for individual realizations of the quenched potential landscape in the Sinai model. The universal localization due to the Golosov effect is seen distinctly. The horizontal black line shows the value 32.

Concurrently, it displays an ageing dependence proportional to $\ln^4(t)/t$, i.e., the process is progressively slowed down. Physically, this is effected when the random walker hits increasingly deeper wells. In figure 1, without fitting, we see excellent agreement between the analytical prediction (7) and the simulations, including the dependence on t.

However, when discussing time averages in nontrivial quenched systems such as a Sinai landscape, we must distinguish between at least two averaging scenarios. In the first case each path is realized on its own unique quenched landscape, and after averaging the individual

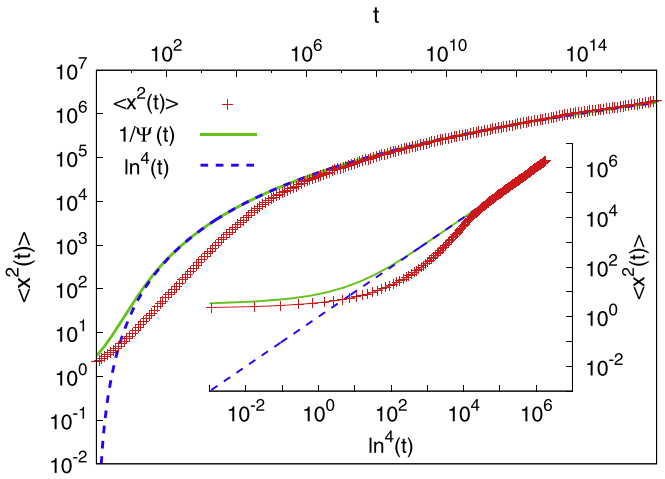

Figure 3. MSD $\langle x^2(t)\rangle$ of the CTRW ($\gamma = 4$, $\tau_0 = \mathrm{e}$, $\langle \delta x^2\rangle = 1$ are used for all CTRW plots). Main graph: log–log scales. Inset: $\langle x^2(t)\rangle$ versus $\ln^4(t)$ with linear asymptote.

time-averaged MSDs $\overline{\delta^2}$ over the disorder we get equation (7). Second, we can consider one unique disordered system with an ensemble of non-interacting particles which all start at the origin. The thermal noise is independent for each particle. Still, in the long time limit we can expect that the time-averaged MSD for all particles will depend on the specific realization of the disorder, and due to the Golosov localization effect all trajectories will yield similar values for the time-averaged MSD. Hence we now focus on the Golosov effect [38]: in a given realization of the disorder, the ratio $\langle x(t)\rangle/\ln^2 t$ for a fixed initial position up to a prefactor of order unity becomes deterministic: the particles get stuck in the deepest potential minimum that they can reach within the time t. In particular, for the standard deviation the result $[\langle x^2(t)\rangle - \langle x(t)\rangle^2]^{1/2} \simeq 32$ in scaled units was obtained [38]. Figure 2 shows that a universal localization of this MSD does indeed emerge. The variations of the onset and height of the plateaus in figure 2 reflect different realizations of the disorder. We emphasize the slow convergence to the Golosov effect, found after 10^4 to 10^5 time steps. While in a simpler map-based system a Golosov-type localization was previously observed numerically [39], to the best of our knowledge this is the first numerical demonstration and analysis of the fundamental Golosov effect in the Sinai model. This observation is thus our second main result.

3. Ultraslow CTRWs

In contrast to systems with quenched disorder, those with annealed disorder are typically amenable to a rigorous treatment. It would therefore be desirable to have a process that captures the essential features of the Sinai diffusion. We show that such a process is given by a renewal CTRW on a one-dimensional lattice with the asymptotic form $\psi(\tau) \sim h(\tau)/\tau$ of the distribution of waiting times τ elapsing between successive jumps [34]. Here $h(\tau)$ is a slowly varying function[5]. Jumps to the left and to the right are equally likely, and the probability that no jump occurs until time t is $\Psi(t) = \int_t^\infty \psi(\tau)\mathrm{d}\tau$, in terms of which we express our results. A typical example is the logarithmic form [26, 32–34]

[5] That is, $h(\mu\tau) \sim h(\tau)$ as $\tau \to \infty$ for $\mu > 0$. For instance, $h(\tau) \sim 1/\ln^\gamma(\tau)$ with $\gamma > 0$

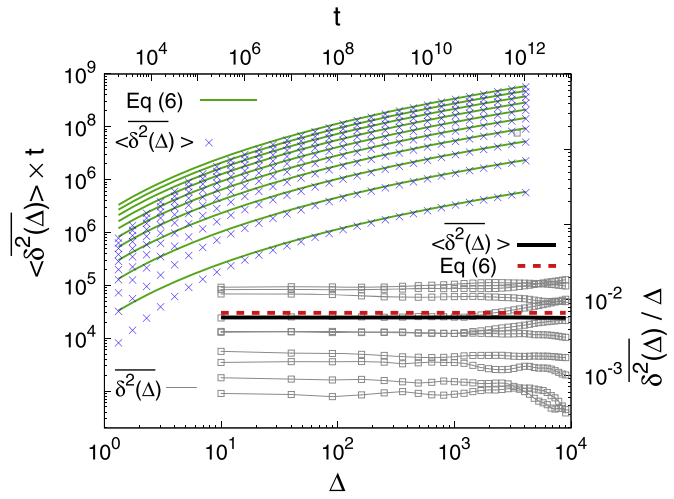

Figure 4. Numerical results for $\langle\overline{\delta^2}\rangle \times t$ for the CTRW versus t for $\Delta = 20$ to 200 in steps of 20 (×, bottom to top). Lines show equation (9), without an adjustable parameter. Bottom right: $\overline{\delta^2}/\Delta$ versus lag time Δ with $t = 10^7$ for ten different realizations, showing distinct amplitude scatter. Thick lines represent equation (9) and the average $\langle\overline{\delta^2}\rangle$ of the ten plotted realizations.

$$\Psi(t) = \ln^{\gamma}(\tau_0)/\ln^{\gamma}(\tau_0 + t), \tag{8}$$

where having $\tau_0 > 0$ avoids a divergence at $t = 0$. The MSD is given by $\langle x^2(t)\rangle \sim \langle \delta x^2\rangle/\Psi(t)$ [37], where $\langle \delta x^2\rangle$ is the variance of the jump lengths [41]. The specific form (8) recovers the MSD (1) with diffusivity $K_\gamma = \langle \delta x^2\rangle/[2\ln^{\gamma}(\tau_0)]$[6] [26, 32, 34], i.e., for $\gamma = 4$, we find a Sinai-like diffusion. Figure 3 demonstrates the convergence of the simulations to the predicted logarithmic behavior. The agreement, including the prefactor, after some 10^6 steps becomes excellent. In the inset of figure 3 we show the linear asymptotic scaling of $\langle x^2(t)\rangle$ as a function of $\ln^4(t)$.

In this CTRW process, the MSD (1) can be rewritten as $\langle x^2(t)\rangle = \langle \delta x^2\rangle\langle n(t)\rangle$ via the average number of jumps $\langle n(t)\rangle$ of the random walker from $t = 0$ up to time t, and thus $\langle n(t)\rangle \sim 1/\Psi(t)$. To calculate $\langle\overline{\delta^2}\rangle$ we need the correlation function $\langle[x(t' + \Delta) - x(t')]^2\rangle$ (see equation (3)). As individual jumps are independent random variables with zero mean, $\langle[x(t' + \Delta) - x(t')]^2\rangle = \langle \delta x^2\rangle[\langle n(t' + \Delta)\rangle - \langle n(t')\rangle]$. The time-averaged MSD is then $\langle\overline{\delta^2}\rangle \simeq \langle \delta x^2\rangle\Delta/[t\Psi(t)]$. For the form (8), we have

$$\left\langle\overline{\delta^2(\Delta)}\right\rangle \sim \langle x^2(t)\rangle\Delta/t. \tag{9}$$

Ultraslow CTRWs thus exhibit weak ergodicity breaking with a linear dependence on Δ, similarly to CTRWs with a power-law form for $\psi(\tau)$ [28, 41, 42] and other processes [6, 43–45]. Equation (9), up to the numerical factor 549/854, equals the relation (7) between $\langle x^2\rangle$ and $\overline{\delta^2}$ for the disorder-averaged Sinai diffusion. This similarity is our third main result.

We plot in figure 4 results from our simulations for the time-averaged MSD, demonstrating the convergence of the numerical results to the expression (9) as a function of the length t of the time series. Figure 4 also depicts the time-averaged MSD as a function of the

[6] We choose the values $\langle \delta x^2\rangle = 1$ and $\tau_0 = \mathrm{e}$.

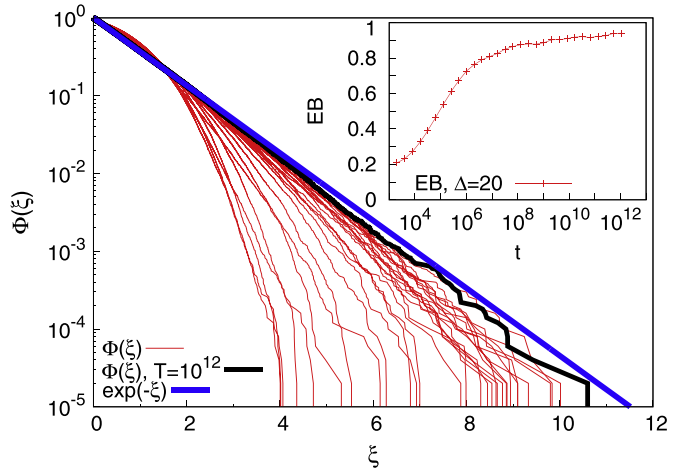

Figure 5. The amplitude scatter distribution $\phi(\xi)$ versus $\xi = \overline{\delta^2}/\langle\overline{\delta^2}\rangle$ for $\Delta = 500$ and increasing t successively approaches the exponential (10) shown by the full line; compare the realization with $t = 10^{12}$. Inset: convergence EB $\to 1$ of the ergodicity-breaking parameter versus t for $\Delta = 20$.

lag time Δ for ten individual realizations, along with the result (9) for the mean behavior. A significant amplitude variation between the individual realizations is observed. This implies that, unlike for Brownian motion, the experimental observation of a single trajectory producing $\overline{\delta^2}$ does not provide the full information on either $\langle x^2\rangle$ or $\langle\overline{\delta^2}\rangle$.

Time averages of physical observables such as the MSD (3) in weakly non-ergodic systems remain random variables even in the limit of long measurement times, but have a well-defined distribution [6, 28, 41, 42, 46]. To derive these fluctuations for the ultraslow CTRW process in terms of the dimensionless variable $\xi = \overline{\delta^2}/\langle\overline{\delta^2}\rangle$, we make use of the relation $\overline{\delta^2(\Delta)}/\langle\overline{\delta^2(\Delta)}\rangle = n(t)/\langle n(t)\rangle$ [42, 47] and invoke the probability for the occurrence of n jumps up to time t, $p_n(s) = [1 - \psi(\tau)]s^{-1}\exp\{n\ln[\psi(s)]\}$ in Laplace space [3]. For the latter, we get after Laplace inversion $p_n(t) \sim \Psi(t)\exp\{-n\Psi(t)\}$. Finally, after carrying out the change of variables $\phi(\xi) = p_n(\xi) \times \mathrm{d}n/\mathrm{d}\xi$, we arrive at the exponential form for the distribution of time averages:

$$\lim_{t\to\infty}\phi(\xi) \sim \exp(-\xi). \tag{10}$$

This result is universal in the sense that it is independent of the specific form of the waiting distribution for ultraslow diffusion. The maximum of $\phi(\xi)$ is at $\xi = 0$, i.e., many realizations of the ultraslow CTRW do not perform any jump. Trajectories with many jumps (larger ξ values) are exponentially suppressed. The ergodicity-breaking parameter [42] is $\mathrm{EB} = \lim_{t\to\infty}\langle\xi^2\rangle - 1 = 1$. The universal fluctuations of ultraslow CTRWs shown in figure 5 are another central result. For Sinai diffusion this point remains open, as our simulations do not provide sufficiently precise traces for analyzing amplitude fluctuations. The results for the Golosov effect (figure 2) show that the simulation times are beyond our reach.

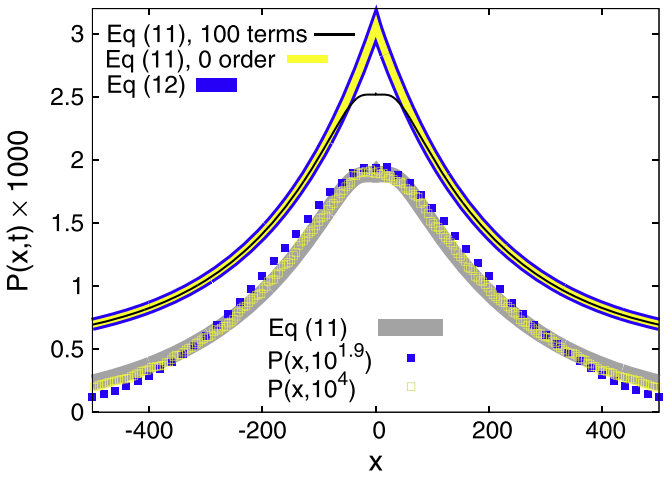

Figure 6. PDF (11) for Sinai diffusion (thick gray line) with numerical results for two times (■ and □), showing good convergence. Shifted curves (top): the rescaled PDF (12) of the ultraslow CTRW (thick blue line) with the zero-order term of the Sinai PDF (11) (medium yellow line) and the result (11) with 100 terms (thin black line), showing perfect agreement of the tails.

4. The similarity of the PDFs

We would expect the PDF $P(x, t)$ to be more sensitive to the deep differences between the CTRW and Sinai diffusion. Figure 6 shows good convergence of the numerical data to the Sinai PDF [48, 49]

$$\widetilde{P(x,\,t)} \sim \frac{4}{\pi^2 \ln^2(t)} \sum_{n=0}^{\infty} \frac{(-1)^n}{2n+1} \exp\left(-\frac{(2n+1)^2 \pi^2 |x|}{4 \ln^2(t)} \right) \tag{11}$$

for increasing t. At all times, the zeroth term of this series contributes ≈0.33 to the normalization. Higher order, alternating terms effect a distinct central plateau, while the wings of the PDF (11) are dominated by the zeroth term. The numerical results nicely corroborate the flat central region of the PDF, which is physically due to the local bias of the Sinai diffusion at each site effecting the small depletion at the origin. We compare in figure 6 the PDF (11) with the CTRW PDF [26, 32, 34]

$$P(x,\,t) \sim \sqrt{\Psi(t) \Big/ \left[2\langle \delta x^2 \rangle \right]} \exp\left\{ -|x| \sqrt{2\Psi(t)/\langle \delta x^2 \rangle} \right\}. \tag{12}$$

As we are interested in the qualitative comparison of the CTRW and Sinai diffusion in equation (11), we rescale the zero-order term with a factor of order unity such that it is identical to the PDF (12) with its distinct cusp at the origin. Figure 6 shows that the full result (11) perfectly matches the tails of the CTRW PDF (12). In the analysis of experimental data, the PDFs of the two processes will be practically indistinguishable unless very accurate data are available.

5. Conclusions

Sinai diffusion and the ultraslow renewal CTRW are fundamentally different: the former takes place in a quenched random potential, the latter in an annealed environment. Despite this difference, they exhibit identical logarithmic scalings of the ensemble MSD and weak ergodicity breaking: the time-averaged MSDs scale linearly with the lag time Δ and explicitly depend on the process time t in a characteristic way. We pointed out the deep connection between the Golosov phenomenon and ergodicity breaking, a topic that demands rigorous mathematical treatment. The fluctuations of the amplitude of the time-averaged MSD for the ultraslow annealed model exhibit a remarkable universality: extended motion recorded in terms of the time-averaged MSD is exponentially suppressed and details of the waiting time distribution do not matter. The importance of the initial conditions, i.e. two particles starting at the same location in the same or distinct realizations of the potential, for the fluctuations of time averages and the commutativity of averages over thermal noise and disorder remain open questions, and are the topics of our current investigations [37]. Our current and future results will be of interest beyond the Sinai model under investigation in the field of strongly disordered systems in the presence of thermal noise.

Acknowledgments

We acknowledge funding from the Academy of Finland (FiDiPro scheme, to RM), Alexander von Humboldt Foundation (AG), Berlin Mathematical Society (AVC), and Israel Science Foundation (EB).

References

[1] Pearson K 1905 *Nature* **72** 294
[2] Einstein A 1905 *Ann. d. Physik* **17** 549
Einstein A 1906 *Ann. d. Physik* **19** 371
von Smoluchowski M 1906 *Ann. d. Physik* **21** 756
[3] Hughes B D 1995 (*Random Walks and Random Environments* Vols 1 and 2) (Oxford, UK: Oxford University Press)
[4] Sornette D 2006 *Critical Phenomena in Natural Sciences* (Berlin: Springer)
[5] Gallager R G 2013 *Stochastic Processes: Theory for Applications* (Cambridge, UK: Cambridge University Press)
Miltov K V and Omney E 2014 *Renewal Processes* (Berlin: Springer)
[6] Metzler R, Jeon J-H, Cherstvy A G and Barkai E 2014 *Phys. Chem. Chem. Phys.* **16** 24128
[7] Bouchaud J-P and Georges A 1990 *Phys. Rep.* **195** 127
Bouchaud J-P, Comtet A, Georges A and Le Doussal P 1990 *Ann. Phys. (N.Y.)* **201** 285
[8] Temkin D E 1972 *Sov. Math. Dokl* **13** 1172
[9] Sinai Ya G 1982 *Theory Prob. Appl.* **27** 256
[10] Oshanin G, Rosso A and Schehr G 2013 *Phys. Rev. Lett.* **110** 100602
Dean D S, Gupta S, Oshanin G, Rosso A and Schehr G 2014 *J. Phys. A: Math. Theor.* **47** 372001
[11] Fisher D S, Le Doussal P and Monthus C 2001 *Phys. Rev.* E **64** 066107
[12] Bruinsma R and Aepply G 1984 *Phys. Rev. Lett.* **52** 1547
[13] de Gennes P G 1975 *J. Stat. Phys.* **12** 463
Oshanin G and Redner S 2009 *Europhys. Lett.* **85** 10008
[14] Waler J-C, Ferrantini A, Carlon E and Vanderzande C 2012 *Phys. Rev.* E **85** 031120
Kafri Y and Polkovnikov A 2006 *Phys. Rev. Lett.* **97** 208104
[15] Mathé J *et al* 2004 *Biophys. J.* **87** 3205
Lubensky D K and Nelson D R 1999 *Biophys. J.* **77** 1824
[16] Kafri Y, Lubensky D K and Nelson D R 2004 *Biophys. J.* **86** 3373

[17] Brummelhuis M J A and Hilhorst H J 1988 *J. Stat. Phys.* **53** 249
Bénichou O and Oshanin G 2002 *Phys. Rev.* E **66** 031101
[18] Juhász R, Santen L and Iglói F 2005 *Phys. Rev. Lett.* **94** 010601
[19] Lomholt M A, Lizana L, Metzler R and Ambjörnsson T 2013 *Phys. Rev. Lett.* **110** 208301
[20] Matan K, Williams R B, Witten T A and Nagel S R 2002 *Phys. Rev. Lett.* **88** 076101
[21] Richard P, Nicodemi M, Delannay R, Ribière P and Bideau D 2005 *Nature Mat.* **4** 121
[22] Boettcher S and Sibani P 2011 *J. Phys. Cond. Mat.* **23** 065103
[23] Schmittmann B and Zia R K P 1999 *Am. J. Phys.* **67** 1269
[24] Afzal N and Pleimling M 2013 *Phys. Rev.* E **87** 012114
[25] Cherstvy A G and Metzler R 2013 *Phys. Chem. Chem. Phys.* **15** 20220
[26] Dräger J and Klafter J 2000 *Phys. Rev. Lett.* **84** 5998
[27] Sanders L P, Lomhotl M A, Lizana L, Fogelmark K, Metzler R and Ambjörnsson T 2014 *New. J. Phys.* (arXiv:1311.3790) at press
[28] Barkai E, Garini Y and Metzler R 2012 *Phys. Today* **65**(8) 29
[29] Miyaguchi T and Akimoto T 2011 *Phys. Rev.* E **83** 031926
[30] Boyer D, Dean D S, Mejia-Monasterio C and Oshanin G 2012 *Phys. Rev.* E **85** 031136
[31] Massignan P *et al* 2014 *Phys. Rev. Lett.* **112** 150603
[32] Havlin S and Weiss G H 1990 *J. Stat. Phys.* **58** 1267
[33] Chechkin A V, Klafter J and Sokolov I M 2003 *Europhys. Lett.* **63** 326
[34] Denisov S and Kantz H 2011 *Phys. Rev.* E **83** 041132
Denisov S I, Yuste S B, Bystrik Yu S, Kantz H and Lindenberg K 2011 *Phys. Rev.* E **84** 061143
[35] Bouchaud J-P 1992 *J. Phys. I (Paris)* **2** 1705
[36] le Doussal P, Monthus C and Fisher D S 1999 *Phys. Rev.* E **59** 4795
[37] Chechkin A V, Godec A, Metzler R, Kantz H and Barkai E (unpublished)
[38] Golosov A O 1984 *Commun. Math. Phys.* **92** 491
[39] Radons G 2004 *Physica D* **187** 3
[40] Metzler R and Klafter J 2000 *Phys. Rep.* **339** 1
[41] Lubelski A, Sokolov I M and Klafter J 2008 *Phys. Rev. Lett.* **100** 250602
Khoury M, Lacasta A M, Sancho J M and Lindenberg K 2011 *Phys. Rev. Lett.* **106** 090602
Sokolov I M, Heinsalu E, Hänggi P and Goychuk I 2009 *Europhys. Lett.* **86** 30009
Magdziarz M and Weron A 2011 *Phys. Rev.* E **84** 051138
Albers T and Radons G 2013 *EPL* **102** 40006
[42] He Y, Burov S, Metzler R and Barkai E 2008 *Phys. Rev. Lett.* **101** 058101
Burov S, Jeon J-H, Metzler R and Barkai E 2011 *Phys. Chem. Chem. Phys.* **13** 1800
[43] Cherstvy A G, Chechkin A V and Metzler R 2013 *New J. Phys.* **15** 083039
Cherstvy A G, Chechkin A V and Metzler R 2014 *Soft Matter* **10** 1591
Fuliński A 2013 *J. Chem. Phys.* **138** 021101
Fuliński A 2011 *Phys. Rev.* E **83** 061140
[44] Thiel F and Sokolov I M 2014 *Phys. Rev.* E **89** 012115
Jeon J-H, Chechkin A V and Metzler R 2014 *Phys. Chem. Chem. Phys.* **16** 15811
Miyagu-chi T and Akimoto T 2011 *Phys. Rev.* E **83** 031926
[45] Tejedor V and Metzler R 2010 *J. Phys. A: Math. Theor.* **43** 082002
Magdziarz M, Metzler R, Szczotka W and Zebrowski P 2012 *Phys. Rev.* E **85** 051103
[46] Bel G and Barkai E 2005 *Phys. Rev. Lett.* **94** 240602
Rebenshtok A and Barkai E 2008 *J. Stat. Phys* **133** 565
[47] Schulz J, Barkai E and Metzler R 2013 *Phys. Rev. Lett.* **110** 020602
Schulz J, Barkai E and Metzler R 2014 *Phys. Rev.* X **4** 011028
[48] Comtet A and Dean D S 1998 *J. Phys. A: Math. Gen.* **31** 8595
Kesten H 1986 *Physica A* **138** 299
[49] Nauenberg M 1985 *J. Stat. Phys.* **41** 803
Bunde A, Havlin S, Roman H E, Schildt G and Stanley H E 1988 *J. Stat. Phys.* **50** 1271